Mitigation of the Antenna Carrier Impact in Dual-Polarized Phased Arrays with Electromagnetic Bandgaps for Airborne SAR Sensors

Diego Lorente[1], Markus Limbach[1], Bernd Gabler[1], Héctor Esteban[2], Vicente E. Boria Esbert[2]
[1]German Aerospace Center (DLR), Microwaves and Radar Institute, Oberpfaffenhofen, Germany, diego.lorentecatalan@dlr.de
[2]Universitat Politècnica de València, Departamento de Comunicaciones, Valencia, Spain

***Abstract*—In this work, the impact of the antenna carrier, an aerodynamic attachment structure that allows the antenna installment on the aircraft, is analyzed. The resulting polarization-dependent edge diffraction effects of a flight-model L-band phased array antenna, embedded in the antenna carrier, is experimentally validated. Measurements show a pattern distortion in the horizontal polarization along with a gain reduction of 1 dB in the elevation plane, in which the beam steering is performed that also corresponds with the E-plane, thus becoming this polarization more sensitive to edge diffraction effects. Further analysis is performed increasing the electrical size of the antenna carrier diameter up to $11\lambda_0$. A low-profile and planar solution, based on Electromagnetic Bandgaps is presented, by which the induced surface currents on the antenna carrier for the horizontal polarization are mitigated, thus reducing the impact of edge diffraction effects without interfering in the performance of the vertical polarization. Thereby, the desired radiation characteristics can be fulfilled regardless of the antenna carrier structure for both polarizations.**

***Index Terms*—Airborne SAR, phased array antenna, dual-linear polarized, antenna carrier, edge diffraction, surface wave, Electromagnetic Bandgaps.**

I. Introduction

Synthetic Aperture Radar (SAR) has become one of the most well established remote-sensing techniques today, and the growing interest in Earth surface monitoring systems reaffirms this trend [1]. In order to support the technological implementation of future spaceborne SAR sensors, airborne SAR systems play a key role, since their operational versatility allow to test new radar concepts and signal processing techniques that are supported by novel hardware developments [2], [3].

The radar antenna design in airborne applications is not only dependent on the limited available antenna aperture size on the aircraft, but also by the mandatory fulfillment of the airworthiness requirements, that determines the antenna installment structure. The mechanical attachment of the antenna on the aircraft, that can be sideways or beneath the fuselage, is implemented by means of a flight-certified holding platform, also known as antenna carrier.

Precisely, due to the propagation nature of the radiated fields and since the antenna is not isolated, it irremediably interacts with its environment. Usually, airborne antennas are surrounded by metallic structures, such as the aircraft or the antenna carrier, onto which surface currents are induced due to fields propagation that extend many wavelengths. The wave interactions with the antenna environment can lead to scattering, multipath interference, or edge diffraction effects from discontinuities on the surrounding geometry.

Thus, the antenna interaction with its environment can lead to a distortion of its electrical performance, causing gain reduction, radiation enhancement at undesired directions or increase of cross-polarization levels. Some well-known approaches to deal with it make use of choke rings [4] or metamaterial absorbers [5]. However, choke rings can become bulky solutions, and the use of microwave absorbers can lead to pattern distortion or loss of desired radiated energy. Other solutions take advantage of the stop-band properties of Electromagnetic Bandgaps (EBGs) to synthesize a high impedance surface ground [6] and suppress the surface wave propagation, thus enhancing the radiation properties of the antenna or to reduce the interference between antenna elements. In addition, due to its miniaturization and integration capabilities, as well as its low-profile realization, EBGs become a suitable solution in order to mitigate the antenna external interactions in airborne applications, thus achieving a radiation performance regardless of the antenna environment.

Usually, edge diffraction effects are analyzed considering individual antennas mounted on finite ground planes [7], evaluating single antenna elements in planar arrays [8], [9], or examining the scanning performance of single-polarized phased array antennas [10]. Only in [11], a dual-polarized phased array for weather radar applications is considered for the analysis of edge diffraccion effects. To the best of author's knowledge, no polarization-dependent beam steering analysis of edge diffraction effects in a dual linear-polarized phased array antenna, considering a real airborne SAR scenario, as presented in this work, has been performed so far.

In this paper, the polarization-dependency impact of the edge diffraction effects, resulting from the interaction of a constructed flight-model phased array antenna with the flight-certified carrier structure is analyzed and experimentally verified. The analysis is extended considering different electrical sizes of the antenna carrier. In addition, a solution to mitigate the antenna interaction with the carrier, based on EBGs, is also proposed and validated with simulations.

This work is organized as follows: in section II, the electri-

cal characteristics of the phased array antenna, along with its mechanical attachment on the aircraft, are described. Then, in section III, the measurements of a flight-model antenna installed on the carrier, and a comparison with the stand-alone configuration, is presented and analyzed for both polarizations. Consequently, the edge diffraction effects are further examined by increasing the electrical size of the antenna carrier. In section IV, a solution to mitigate the antenna interaction with the carrier using EBGs, is presented. Finally, the outcome of the proposed work is discussed in section V.

II. Antenna aircraft installment

The airborne SAR antenna is a dual-linear polarized L-band planar phased array of 5×8 elements operating at 1.325 GHz and with a bandwidth of 200 MHz [12]. A beam steering in elevation at 42° is performed to achieve the side-looking operation of airborne SAR systems. In addition, an amplitude tapering is implemented in both principal planes, in order to improve the antenna side-lobe level and reduce radar ambiguities. The array elements, along with the feeding networks, are integrated within a housing structure, achieving an extremely compact antenna assembly, that enables its mechanical attachment onto the antenna carrier, as depicted in Fig. 1. The antenna aperture is approximately 85.5 cm × 53 cm, being the XZ and YZ planes, the elevation and azimuth directions respectively, by which in SAR systems, the azimuth derection determines the flight path. As convention, the E-plane of the horizontal and vertical polarization coincide with the XZ and YZ plane, respectively. The measured antenna gain without the carrier (stand-alone configuration), is 14.9 dB for the horizontal polarization and 15.1 dB for the vertical one.

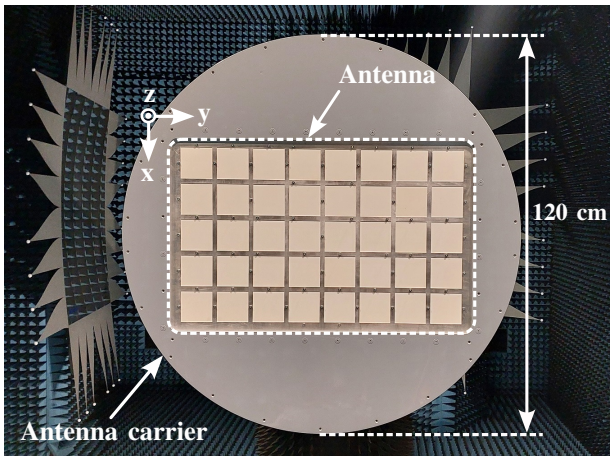

Fig. 1. Antenna installed on the carrier structure during a measurement in the DLR's Compact Test Range.

The antenna carrier is a Carbon-Fiber Reinforced Polymer (CFRP) circular plate with diameter 120 cm and thickness 1.27 cm. Its surface is covered with a copper mesh, thus being conductive. The antenna carrier, along with a rotation platform, allows several ground footprints or illumination configurations under different looking angles, thus maximizing the retrieval of information for bistatic radar systems. The installment position and the supporting holding structure on the aircraft Dornier Do-228 is shown in Fig. 2.

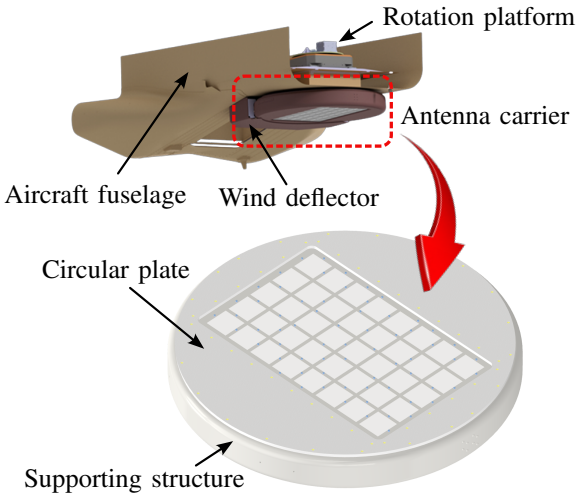

Fig. 2. Antenna installment under the aircraft fuselage by means of the antenna carrier platform.

III. Edge diffraction effects

The radiation pattern of the antenna embedded in the carrier structure, as depicted in Figure 1, is measured in the Compact Test Range of the German Aerospace Center, and compared with the stand-alone configuration, in which only the antenna itself is measured. The co-polar and cross-polar levels in elevation for both polarizations are plotted in Fig. 3.

It can be noted that, for the horizontal polarization and when the antenna is installed on the carrier, the main beam is widened, leading to a gain reduction of 1 dB. This gain decrease has to be considered twice in the system performance, since due to the two-way operation of SAR systems, the same antenna is used for both transmission and reception purposes. On the other side, the radiation pattern of the vertical polarization remains practically unaltered, regardless the mounting of the antenna carrier.

In order to examine the polarization-dependency impact of the antenna carrier on each polarization, the magnitude of the surface currents that are induced on the carrier surface are plotted in Fig. 4. This analysis is performed using the full-wave electromagnetic simulation software HFSS.

It can be seen that, for the horizontal polarization, the intensity of the surface currents induced on the surface carrier is considerably stronger than for the vertical one. In addition, they propagate along the carrier surface, unlike the vertical polarization, that are more concentrated around the antenna aperture. This is explained since, due to the metallic surface of the antenna carrier, the radiated electric field propagates along the antenna carrier surface, which supports TM surface waves that interact with the edges or discontinuities, leading to edge diffraccion effects, as depicted in Fig. 5.

The resulting scattered field from the edges and corners is added to the direct antenna radiated field, producing constructively or destructively interferences that can distort the

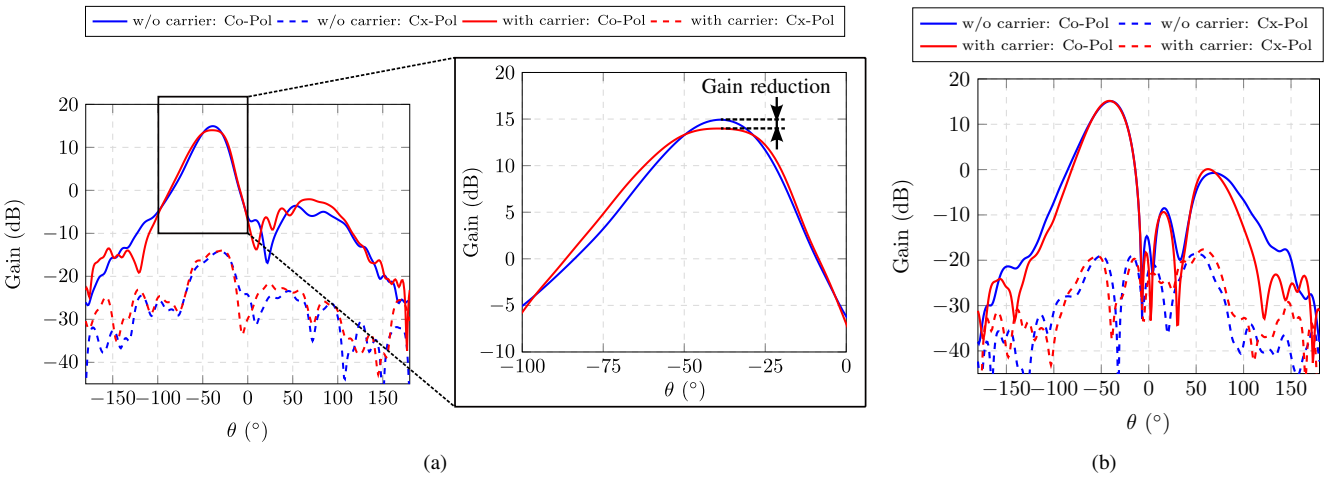

Fig. 3. Measured co-polar and cross-polar levels in elevation with and without the antenna carrier at 1.325 GHz. (a) Horizontal pol. (b) Vertical pol.

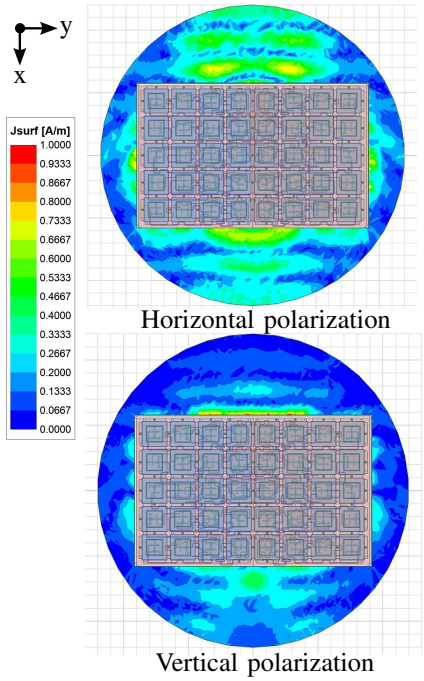

Fig. 4. Magnitude of the surface currents that are induced on the antenna carrier. Each polarization is excited by the same input power.

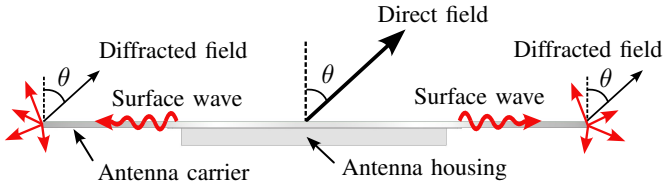

Fig. 5. Surface waves induced on the antenna carrier surface.

radiation pattern. This impact is especially visible in angular regions of low field intensitiy such as backward radiation, side lobe level or radiation nulls, as well as it may also increase the cross-polarization levels. In addition, the edge diffraction effect can also distort the main beam of the antenna pattern, especially in the E-plane, causing an amplitude ripple. Since the elevation plane (XZ), where the beam steering occurs, corresponds to the E-plane of the horizontal polarization, in which the electrical size of the antenna structure is increased due to the carrier plate, the impact of the edge diffraction is more visible for this polarization, as measurements show. On the contrary, for the vertical polarization that is orthogonal to the horizontal one, the elevation plane corresponds to the H-plane, thus being less sensitive to this effect.

Fig. 6 shows the propagation of the radiated electric fields in the elevation plane. It can be noted the propagation of the radiated fields along the carrier surface for the horizontal polarization, unlike the vertical one.

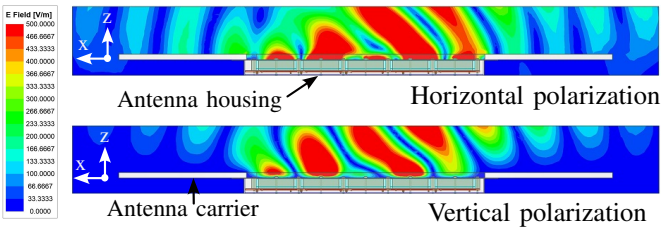

Fig. 6. Propagation of the radiated fields along the antenna carrier surface in the elevation plane. Each polarization is excited by the same input power.

A further analysis of the edge diffraction effect is performed considering larger electrical sizes of the antenna carrier. Fig. 7 plots the simulated radiation pattern in elevation for the horizontal polarization, when the antenna carrier radio is increased 50% and 100%, corresponding to values of 90 cm and 120 cm, respectively, and compared with the original radio of 60 cm.

It can be seen that increasing the antenna carrier diameter considerably distorts the main beam of the horizontal polarization, leading to an amplitude ripple. This is caused by the increase of the metallic surface structure along the E-plane of the horizontal polarization, by which surface waves propagate and the edge effects become more noticeable, as previously

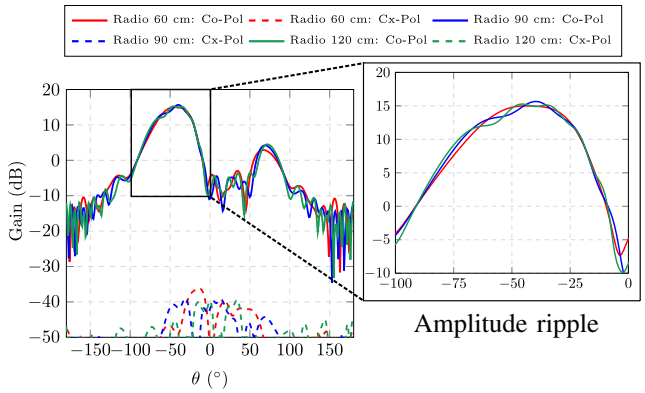

Fig. 7. Edge diffraction analysis for different electrical sizes of the antenna carrier at 1.325 GHz. Horizontal polarization.

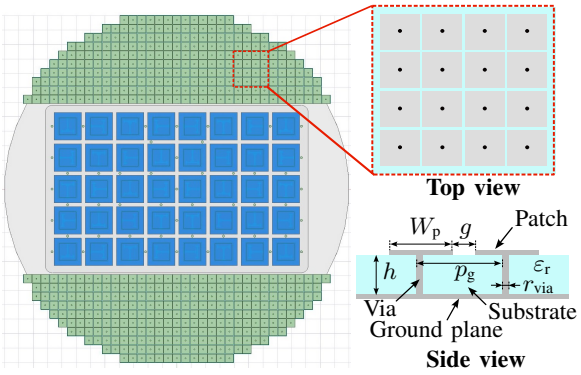

Fig. 8. Simulated antenna structrure with EBGs placed on the carrier.

explained. On the other side, the performance of the vertical polarization remains practically unaltered. It can be noted that the simulated gain is slightly higher than the measured with the carrier, as well as the cross-polarization levels are lower, due to feeding network losses and the required measurement sensitivity, respectively.

The polarization-dependent edge diffracion effect, due to the carrier geometry, has to be compensated in order to achieve a more comparable radiation performance for both polarizations, that has a direct impact on the SAR system operation.

IV. Mitigation of the Edge Diffraction Effects by Means of Electromagnetic Bandgaps

A possible solution to mitigate the antenna interaction with the carrier comprises the use of Electromagnetic Bandgaps (EBGs), by which the propagation of surface waves can be suppressed, thus reducing the edge diffraction effects. EBGs are metal-dielectric structures that are periodically arranged along a two-dimensional pattern by the repetition of the same unit cell. Due to its low-profile and planar implementation they become a compact and suitable solution for airborne applications, where a high degree of integration is required.

One of the most well-known unit cell (UC) design is the mushroom type. Further unit-cells design can be considered for broadband or multiband applications. Nevertheless, for the presented work, the mushroom type UC is used as a proof-of-concept to validate the proposed approach.

The mushroom type EBG-UC is a metallic patch placed on a substrate and connected to the ground with a via. Each square patch has a width W_p and is separated to the next element by a gap g, becoming the unit-cell periodicity $p = W_\mathrm{p} + g$. The via stub, whose height is determined by the substrate thickness h, has a radio r_via. A capacitance C is formed by the gap between patches, and an inductance L results from the current loop generated among the patches and vias, leading to an equivalent LC parallel resonant circuit whose frequency of resonance is given by $f_0 = \frac{1}{2\pi\sqrt{LC}}$, where no surface wave propagates.

Fig. 8 shows the EBGs mushroom type placed on the carrier surface. The unit-cell is optimized to provide a bandgap approximately centered at the antenna frequency of operation 1.325 GHz. In order to characterize the stop-band, where no surface wave propagates, an eigenmode solver of the unit cell with periodic boundaries is simulated in HFSS, and the dispersion diagram within the Brillouin zone is analyzed. The unit cell is implemented using a substrate Rogers TMM4 ($\varepsilon_\mathrm{r} = 4.5$, $tan\delta = 0.002$), and designed with the geometrical parameters listed in Table I.

TABLE I
Geometrical Parameters of the Mushroom Type EBG.

W_p	28.5 mm	g	2 mm	r_via	2 mm	h	8 mm

The simulated dispersion diagram is plotted in Figure 9. The bandgap, that is given by the intersection of the two first propagating modes with the light line, approximately corresponds to the frequency range between 1.15 GHz∼1.55 GHz, which also covers the antenna operational bandwidth. In this frequency band, no real wavenumber solution exists, and thus no surface wave propagates.

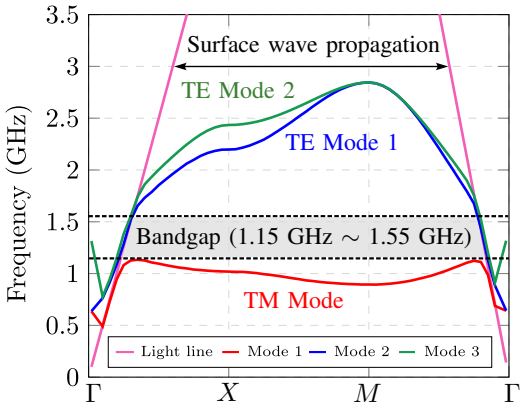

Fig. 9. Calculated dispersion diagram.

Fig. 10 shows the magnitude of the surface currents on the carrier structure and the radiated electric field for the horizontal polarization. It can be clearly seen that the intensity of the induced currents is strongly reduced, as well as that the radiated fields do not propagate along the carrier surface, thus enhancing the isolation of the antenna with the carrier. A

comparison of the radiation pattern in elevation of the antenna installed on the carrier with and without the EBGs is plotted in Fig. 11. Due to the EBGs, no beam distortion occurs as well as the antenna gain is increased by 1 dB approximately. The performance of the vertical polarization is not altered, since the surface current distribution is more concentrated around the antenna aperture, and the position of the EBGs is set to influence mostly the horizontal polarization. Thus, the use of EBGs allows to achieve a more independent antenna performance, considering not only to the given antenna carrier geometry, but also larger electrical carrier sizes.

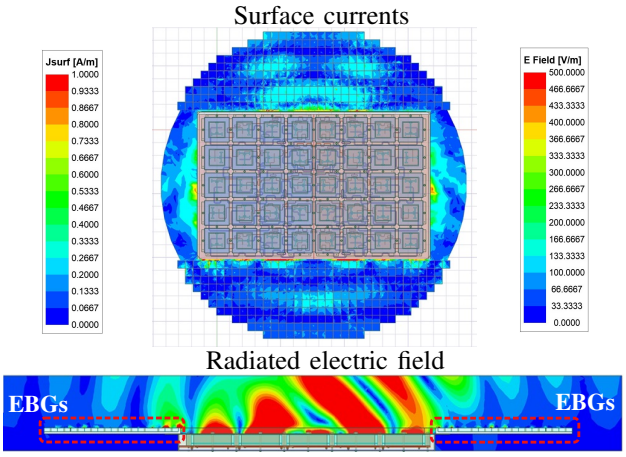

Fig. 10. Surface currents and radiated electric field with EBGs. Horizontal polarization.

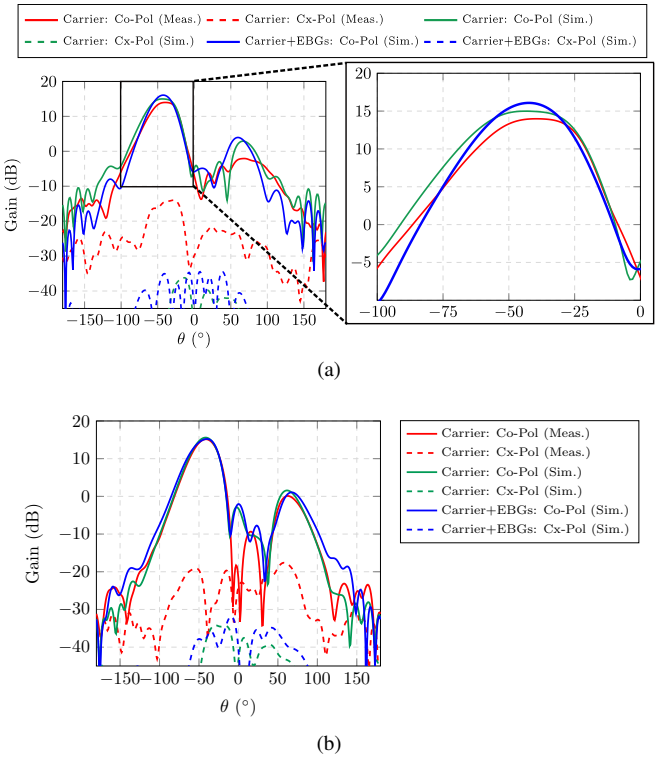

Fig. 11. Analysis radiation pattern in elevation with and without EBGs at 1.325 GHz. (a) Horizontal polarization. (b) Vertical polarization.

V. Conclusion

In this paper, the polarization-dependent edge diffraction effects, due to the antenna carrier interaction in airborne SAR sensors, has been examined. The analysis has been performed considering a manufactured flight-model dual-linear polarized L-band phased array antenna, with a flight-certified antenna carrier structure, and experimentally verified with measurements. A solution to mitigate the antenna carrier interaction, making use of the surface wave suppression characteristics of EBGs, is presented, by which the impact of the carrier is reduced for the horizontal polarization, while for the vertical one remains unaffected. The proposed approach allows to achieve a more balanced electrical performance for both polarizations regardless the antenna environment, especially relevant for airborne applications. In addition, the presented solution can be extended to multifrequency airborne SAR systems, where several antennas, operating at different frequencies for interferometric purposes, are installed on the same carrier structure on the aircraft.

References

[1] S. Huber, F. Q. de Almeida, M. Villano, M. Younis, G. Krieger and A. Moreira, "Tandem-L: A technical perspective on future spaceborne SAR sensors for earth observation," IEEE Transactions on Geoscience and Remote Sensing., vol. 56, no. 8, pp. 4792-4807, Aug. 2018.

[2] R. Horn, M. Jaeger, M. Keller, M. Limbach, A. Nottensteiner et al., "F-SAR - recent upgrades and campaign activities," Proc. 2017 18th International Radar Symposium (IRS), Prague, Czech Republic, 2017.

[3] A. Reigber, E. Schreiber, K. Trappschuh, S. Pasch, G. Müller, et al., "The high-resolution digital-beamforming airborne SAR system DBFSAR," Remote Sensing, vol. 12, no. 11, May. 2020.

[4] D. Lin, E. Wang, and J. Wang, "New choke ring design for eliminating multipath effects in the GNSS system," International Journal of Antennas and Propagation, vol. 2022, no. 1, 2022.

[5] S. Caizzone, R.A. Gerguis, E.O. Addo, S.P. Hehenberger, and W. Elmarissi, "Spatial filtering of multipath at GNSS reference stations through metamaterial-based absorbers," IEEE. Trans. Aeorospace and Electronics Systems, vol. 59, no. 6, pp. 7764-7771, Dec. 2023.

[6] D. Sievenpiper, R. Broas and E. Yablonovitch, "Antennas on high-impedance ground planes," IEEE MTT-S International Microwave Symposium Digest, vol.3, pp. 1245-1248, 1999.

[7] N.A. Aboserwal, C. Balanis, and C.R. Birtcher, "Impact of finite ground plane edge diffractions on radiation patterns of aperture antennas," Progress In Electromagnetics Research B, vol.55, pp. 1-21, 2013.

[8] J. L. Salazar, N. Aboserwal, J. D. Díaz, J. A. Ortiz and C. Fulton, "Edge diffractions impact on the cross polarization performance of active phased array antennas," IEEE International Symposium on Phased Array Systems and Technology (PAST), pp. 1-5, 2016.

[9] S. Srivastava, S. M. S and A. R. Harish, "Mitigating radiation pattern ripples due to edge diffraction in central element of a large array using top hat loaded high impedance surface," 2024 IEEE International Symposium on Antennas and Propagation, Firenze, Italy, 2024, pp. 2649-2650.

[10] T. Lan, Q. Li, Y. Dou, and X. Jiang, "A study of a wide-angle scanning phased array based on a high-impedance surface ground plane," International Journal of Antennas and Propagation, vol. 2019, no. 1, 2019.

[11] J.A. Ortiz, "Impact of edge diffraction in dual-polarized phased array antennas" Ph.D. thesis, School of Electrical and Computer Engineering, University of Oklahoma, EEUU, 2020. [Online]. Available: https://shareok.org/handle/11244/325369.

[12] D. Lorente, M. Limbach, B. Gabler, H. Esteban and V. E. Boria, "Highly integrated low-profile multilayer dual-polarized phased array antenna with truncated cavities for first pulsed bistatic L-band airborne SAR sensor," IEEE Access, vol. 12, pp. 435-449, 2024